

Original Article



# Increased Inflammatory Responses in Patients With Active Disseminated Non-Tuberculous Mycobacterial Infection and High Anti-Interferon-Gamma Autoantibodies

OPEN ACCESS

Received: Jul 16, 2024  
Revised: Aug 21, 2024  
Accepted: Sep 6, 2024  
Published online: Oct 8, 2024

\*Correspondence to

Arnone Nithichanon

Department of Microbiology, Faculty of Medicine and Research and Diagnostic Center for Emerging Infectious Diseases (RCEID), Khon Kaen University, 123 Village No. 16 Mittraphap Road, Nai-Muang, Muang District, Khon Kaen 40002, Thailand.  
Email: arnoni@kku.ac.th

Copyright © 2024. The Korean Association of Immunologists

This is an Open Access article distributed under the terms of the Creative Commons Attribution Non-Commercial License (<https://creativecommons.org/licenses/by-nc/4.0/>) which permits unrestricted non-commercial use, distribution, and reproduction in any medium, provided the original work is properly cited.

ORCID iDs

Pattaraporn Srisai <https://orcid.org/0009-0006-8182-1776>  
Chanchai Hongsa <https://orcid.org/0009-0009-3782-2108>  
Yothin Hinwan <https://orcid.org/0009-0001-3725-7075>  
Varis Manbenmad <https://orcid.org/0009-0003-2828-8974>  
Ploenchan Chetchotisakd <https://orcid.org/0000-0001-9501-5827>  
Siriluck Anunnatsiri <https://orcid.org/0000-0002-6772-4957>

Pattaraporn Srisai <sup>1,2</sup>, Chanchai Hongsa <sup>1,2</sup>, Yothin Hinwan <sup>1,2</sup>,  
Varis Manbenmad <sup>1,2</sup>, Ploenchan Chetchotisakd <sup>3</sup>, Siriluck Anunnatsiri <sup>3</sup>,  
Kiatchai Faksri <sup>1,2</sup>, Todsapol Techo <sup>4</sup>, Kanin Salao <sup>5</sup>, Steven W. Edwards <sup>6</sup>,  
Arnone Nithichanon <sup>1,2,\*</sup>

<sup>1</sup>Department of Microbiology, Faculty of Medicine, Khon Kaen University, Khon Kaen 40002, Thailand  
<sup>2</sup>Research and Diagnostic Center for Emerging Infectious Diseases (RCEID), Khon Kaen University, Khon Kaen 40002, Thailand  
<sup>3</sup>Department of Medicine, Faculty of Medicine Khon Kaen University, Khon Kaen 40002, Thailand  
<sup>4</sup>Department of Biology, Faculty of Science, Khon Kaen University, Khon Kaen 40002, Thailand  
<sup>5</sup>Department of Physiology, Yong Loo Lin School of Medicine, National University of Singapore, 119077 Singapore  
<sup>6</sup>Institute of Infection, Veterinary and Ecological Sciences, University of Liverpool, Liverpool L69 7ZX, United Kingdom

## ABSTRACT

Adult-onset immunodeficiency (AOID) is associated with the presence of anti-IFN- $\gamma$  autoantibodies (auAbs). In disseminated nontuberculous mycobacterial (dNTM) infection with AOID, neutralization of IFN- $\gamma$  by auAb may play a role in disease susceptibility, but other molecular mechanisms are likely to contribute. In this study, dNTM patients, including inactive, active but non-progressive and active, progressive cases were enrolled to measure plasma anti-IFN- $\gamma$  auAb by ELISA and underwent whole-blood RNA sequencing. Healthy control individuals were also enrolled. Plasma IL-8 was then quantified to confirm transcriptomic analysis. Results revealed that anti-IFN- $\gamma$  auAb titers were significantly increased in patients with active stage of disease. Gene expression could separate patients with active infection from individuals with no signs of infection (inactive patients and healthy controls). In active cases, there was over-expression of inflammatory pathways and under-expression of type-2 immunity pathways. Interestingly, increased levels of plasma IL-8 ( $p=0.0167$ ) not only confirmed gene expression results but also correlated with the presence of neutrophilic dermatitis ( $p=0.0244$ ). In conclusion, our findings highlight the value of anti-IFN- $\gamma$  auAb titers for predicting disease reactivity and first propose IL-8 as a promising mediator to be further explored, given its correlation with skin reactive disease, a hallmark of active dNTM infection.

**Keywords:** Autoantibody; Interferon-gamma; Transcriptome; Immunodeficiency; Nontuberculous mycobacteria; Interleukin-8

Kiatichai Faksri 

<https://orcid.org/0000-0001-5022-4182>

Todsapol Techo 

<https://orcid.org/0000-0002-2083-1456>

Kanin Salao 

<https://orcid.org/0000-0003-4731-9556>

Steven W. Edwards 

<https://orcid.org/0000-0002-7074-0552>

Arnone Nithichanon 

<https://orcid.org/0000-0001-5617-8746>

### Conflict of Interest

The authors declare no potential conflicts of interest.

### Abbreviations

AOID, adult-onset immunodeficiency; ARG1, arginase-1; auAb, autoantibody; CPM, counts per million; DAMP, damage-associated molecular pattern; DEG, differentially expressed gene; dNTM, disseminated nontuberculous mycobacterial; GO, Gene Ontology; GPCR, G-protein coupled receptor; HSP, heat shock protein; IQR, interquartile range; NA, data not available; ND, neutrophilic dermatosis; NLRP3, NLR family pyrin domain containing 3; NTM, nontuberculous mycobacteria; PCA, principle component analysis; RNA-seq, RNA sequencing; TCF, T-cell factor.

### Author Contributions

Conceptualization: Chetchotisakd P, Anunnatsiri S, Faksri K, Salao K, Edwards SW, Nithichanon A; Formal analysis: Srisai P, Hinwan Y, Techo T, Nithichanon A; Funding acquisition: Chetchotisakd P, Faksri K, Nithichanon A; Investigation: Hongsa C, Manbenmad V, Chetchotisakd P, Anunnatsiri S, Nithichanon A; Methodology: Hongsa C, Manbenmad V, Chetchotisakd P, Anunnatsiri S, Nithichanon A; Supervision: Chetchotisakd P, Anunnatsiri S, Faksri K, Salao K, Edwards SW, Nithichanon A; Validation: Hongsa C, Manbenmad V, Chetchotisakd P, Anunnatsiri S, Nithichanon A; Visualization: Srisai P, Hinwan Y, Techo T, Nithichanon A; Writing - original draft: Srisai P, Nithichanon A; Writing - review & editing: Srisai P, Hongsa C, Hinwan Y, Manbenmad V, Chetchotisakd P, Anunnatsiri S, Faksri K, Techo T, Salao K, Edwards SW, Nithichanon A.

## INTRODUCTION

Nontuberculous mycobacteria (NTM) can cause opportunistic infections (1). NTM pulmonary disease, the most common condition, is primarily seen in patients with underlying lung diseases (2). However, in immunocompromised hosts, for example in patients with AIDS caused by HIV, extrapulmonary as well as disseminated nontuberculous mycobacterial (dNTM) infection are often seen (3). Among dNTM patients with undetectable HIV, a feature of the disease is the presence of blood circulating autoantibodies (auAb) against IFN- $\gamma$ , which is strongly associated with adult-onset immunodeficiency (AOID) (4,5).

Circulating anti-IFN- $\gamma$  auAb can neutralize many of the functions of IFN- $\gamma$  resulting in increased susceptibility to infections with intracellular pathogens, particularly NTM (6-8), but the function of these Abs in the pathogenesis of dNTM infection is unknown. While ELISA can be used to measure circulating levels of the Abs, assays such as STAT1 phosphorylation are required to determine their functional properties (9,10). We previously reported that measurement of circulating anti-IFN- $\gamma$  auAb inhibitory titer is useful for diagnosis of dNTM and also could be used as a monitoring tool for disease activity (10,11).

Most patients have long-term NTM infections, and some are unresponsive to antimicrobial treatment and experience progressive clinical outcomes (12). The dNTM infections in those with AOID often require hospitalization and death rates are high even after receiving antimycobacterial chemotherapy or immunotherapy (12,13). It is therefore difficult to predict disease progression after therapy, so understanding host responses at different stages of the disease is important to understand mechanisms and to improve disease outcomes.

This study aimed to determine if levels of circulating anti-IFN- $\gamma$  auAb, and transcriptome profiles, in dNTM patients could help stratify patients with different clinical characteristics. Differences in anti-IFN- $\gamma$  auAb titers before and after receiving treatment were compared in dNTM patients with different outcomes. RNA sequencing (RNA-seq) of whole-blood samples of representative healthy individuals and each cohort of dNTM patients was conducted to explore gene expression patterns. Blood transcriptomic analysis has been proven to provide remarkable insights across many infectious, non-infectious and inflammatory diseases (14-17), as well as offering reliable performance in discriminating patients with different disease stages (18,19). In this study, our bioinformatic analyses successfully revealed pathways associated with immunopathogenesis of dNTM infection and these findings were subsequently confirmed by a measurement of the most relevant mediator in plasma. Our findings highlight the value of anti-IFN- $\gamma$  auAb titers for monitoring and predicting disease reactivity. Importantly, we propose IL-8 as a key mediator possibly contributing to reactive skin disorders, such as Sweet syndrome (1,20), a hallmark of active dNTM infection with AOID.

## MATERIALS AND METHODS

### Sample enrollment and definitions

Patients with a history of dNTM infection were recruited in this study from May 2022 to February 2023 at Srinagarind Hospital, Khon Kaen University, Thailand. Ethics approval for the research protocol was reviewed by the Institutional Review Board of Khon Kaen University (HE651152) in compliance with the Declaration of Helsinki. Written informed consent was obtained from all participants prior to collection of peripheral whole blood into

6-ml-heparinized tubes. Each heparinized whole-blood sample was centrifuged at 3,500 rpm for 10 min to separate plasma from blood cells. The collected plasma samples were stored at  $-80^{\circ}\text{C}$  until the measurements of anti-IFN- $\gamma$  auAb and IL-8 were performed. Plasma-depleted whole-blood samples were immediately used for total RNA isolation.

The dNTM infection was defined by either NTM blood culture positive or the presence of NTM infection in more than one organ, with reactive skin disorders such as Sweet syndrome, pustular psoriasis, generalized pustulosis, or erythema nodosum. Cases with concurrent or subsequent opportunistic infections were included. Cases with NTM infection confined solely to the lung, HIV positive and nosocomial infections were excluded (1,10,21). The dNTM patients were divided among several subgroups. Patients with “Inactive Infection” were those who had no signs of infection and had discontinued anti-mycobacterial treatment during the previous 30 days from the day of sample collection, but still required intermittent monitoring. The “Active Infection” cohort included patients who required oral and/or intravenous anti-microbial drugs to control progression of their disease during the previous 30 days from the day of sample collection (10). The “Active Infection” group was then classified into 2 categories; “Non-progressive,” who had stable disease symptoms and continued receiving anti-microbial treatment without requiring hospitalization during the previous 12 months, or “Progressive,” if they experienced worsening clinical outcomes after treatment and required hospitalization during past 12 months (13,22).

Surplus plasma samples of dNTM patients taken at the day of initial diagnosis from routine service at Srinagarind Hospital, Khon Kaen University, Thailand, were paired with their own subsequent samples collected at the current enrollment to examine the dynamic changes of anti-IFN- $\gamma$  auAb titers over the following years. The time elapsed since the initial diagnosis varied among samples, but all were within the 5-year period. Healthy individuals with no detectable indicators of infection were enrolled as a control cohort in accordance with guidelines for the management of blood and blood components of the Blood Transfusion Center, Srinagarind Hospital.

#### Measurement of anti-IFN- $\gamma$ auAb from human plasma samples

Heparinized plasma samples were thawed from  $-80^{\circ}\text{C}$  and ELISA used to quantify anti-human-IFN- $\gamma$  Ab level as inhibitory titer units. The detailed technique protocols have been published previously (10,11,13,21). Briefly, recombinant human IFN- $\gamma$  (BD Biosciences, Franklin Lakes, NJ, USA) at a final concentration of 300 pg/ml was incubated with serially diluted heparinized plasma for 1 h at  $37^{\circ}\text{C}$  to allow plasma anti-IFN- $\gamma$  Ab binding with the recombinant IFN- $\gamma$ . The level of free IFN- $\gamma$  in the incubation mixture was then determined by a human IFN- $\gamma$  ELISA kit (BD OptEIA; BD Biosciences), following the manufacturer’s instructions. The reported inhibitory titer of the anti-human-IFN- $\gamma$  auAb was the lowest dilution of plasma where IFN- $\gamma$  resulted in  $>50\%$  binding (the plasma dilution which an IFN- $\gamma$  level below 150 pg/ml was first observed).

#### Quantification of plasma IL-8

Thawed heparinized plasma samples were subjected to measure concentrations of IL-8 using an IL-8 Human ELISA Kit (BD OptEIA; BD Biosciences), following the manufacturer’s instructions.

### Total RNA purification from human whole-blood samples

Plasma-depleted whole-blood samples were subjected to total RNA isolation using the QIAamp RNA Blood Mini Kit (Qiagen, Valencia, CA, USA), following the manufacturer's protocol. Purified RNA samples were kept frozen at  $-80^{\circ}\text{C}$  before undergoing transcriptomic profiling at the Omics Science and Bioinformatics Center, Chulalongkorn University, Thailand.

Total RNA concentration was measured using DeNovix fluorimeter (DeNovix, Wilmington, DE, USA). Sample purity was checked using Nanodrop (Thermo Fisher Scientific, Waltham, MA, USA) and integrity of the total RNA was assessed using an Agilent 2100 Bioanalyzer (Agilent Technologies, Inc., Santa Clara, CA, USA).

### RNA-Seq library construction and sequencing

Five representative healthy individuals and five patients from each dNTM cohort were randomly selected for RNA-seq analysis. Approximately 500 ng total RNA from each sample was used to create individually indexed strand-specific RNA-Seq libraries by using QIAseq Stranded mRNA Library kits (Qiagen). The reactions were subjected to fragmentation and cDNA synthesis and then QIAseq Beads (Qiagen) were used to separate the cDNAs from the reaction mixtures. Indexing adapters were ligated to the cDNAs, and all cDNA libraries were subsequently inspected for quality by Agilent 2100 Bioanalyzer (Agilent Technologies, Inc.) and quantified using a DeNovix fluorimeter (DeNovix). The indexed sequencing libraries were pooled in equimolar quantities and subjected to cluster generation, followed by paired-end 150-nucleotide read sequencing on an Illumina HiSeq sequencer (Illumina Inc., San Diego, CA, USA).

### Bioinformatic analysis

Raw-read data files were subjected to quality assessment using FASTQC software. Adapter and poor-quality reads were removed using Fastp and Trimmomatic version 0.38 (23). For quality control of raw data, base calling was performed using Illumina RTA software (Illumina Inc.). Demultiplexing was performed by Illumina bcl2fastq 2.17 software based on index information including the number of reads at 5.0 Gb (range, 2.6–7.7) and quality score (Q30) at 84.5% (ranged, 76.8%–89.8%).

After the quality assessment, the fastq files were used as input for mapping using HISAT2 version 2.2.1 (24) which used *Homo sapiens* GRCh38 (accession No. GCA\_000001405.28) as reference (25). To obtain raw gene-count data, featureCounts (26) and htseq version 2.0.2 (27) were used. R studio package DESeq2 was used for the transcript counts (28). Package ComplexHeatmap for heatmap visualization (29) and package EnhancedVolcano for volcano-plots by statistical determination of p-value  $<0.01$  and fold change cut-off at 1.5 (available from: <https://github.com/kevinblighe/EnhancedVolcano>) were subsequently used. A flow chart of this methodology is shown in **Supplementary Fig. 1**.

To further identify the enrichment of Gene Ontology (GO) terms and Reactome pathways, enrichment analysis and visualization were performed using ClusterProfiler (30). The GO terms and Reactome pathways were obtained from org.Hs.eg.db package for human genome-wide annotation (available from: <https://bioconductor.org/packages/org.Hs.eg.db/>) and ReactomePA (31), respectively.

### Estimation of cell-type fractions using CIBERSORTx

To estimate cell-type fractions in bulk whole-blood RNA-seq data, we employed a computational deconvolution approach using CIBERSORTx. Raw gene count data were transformed to counts per million (CPM) using edgeR (32). The CPM-normalized data were filtered to exclude non-expressed genes and those lacking gene symbols. The filtered dataset was then analyzed using the web-based CIBERSORTx tool (33), with batch correction enabled. We utilized the LM22 signature matrix, which comprises 547 marker genes for 22 distinct human hematopoietic cell phenotypes, to determine the proportion of each cell type in individual transcriptome samples (34).

### Data analysis

Statistical tests and visualization were performed using GraphPad Prism version 9.5.1 (GraphPad Software, San Diego, CA, USA) and R studio version 4.3.0. Data were assessed for their normal distribution using the D’Agostino & Pearson test. Comparisons of non-normally distributed data were performed using Kruskal-Wallis tests. Comparisons of paired samples were performed using one-tailed paired t-tests.  $\chi^2$  test was applied to assess the significant differences of categorical data.

## RESULTS

### Significantly higher anti-IFN- $\gamma$ auAb inhibitory titers in active dNTM infection compared to those with inactive infection

Fifty-eight participants including 11 healthy controls and 47 dNTM-infected patients with AOID were recruited in this study. Based on their clinical histories, there were 17 “Inactive Infection”; 15 “Non-progressive Active” and 15 “Progressive Active” cases among the dNTM-infected patients. General characteristics of our participants are shown in **Table 1**. There were no significant differences in terms of the age range, proportion of females/males or occurrence of underlying conditions. Anti-IFN- $\gamma$  auAb was undetectable in all healthy controls, as expected. Anti-IFN- $\gamma$  auAb was detected in 14/17 (82.4%) of inactive dNTM cases and in all active dNTM cases (**Table 1**).

Deeper analysis of our data showed significantly elevated levels of plasma anti-IFN- $\gamma$  auAb in the plasma of patients with active dNTM infection, compared to those with inactive infection

**Table 1.** General characteristics of all participants in this study

Parameters	Healthy controls (n=11)	dNTM patients (n=50)		p-value	
		Inactive Infection (n=17)	Non-progressive Active (n=15)		Progressive Active (n=15)
Age (years)	51.8±2.5	64.3±3.8	56.9±1.9	54.1±5.1	n.s.*
Number of females	8 (72.7)	10 (58.8)	7 (46.7)	10 (66.7)	n.s.†
Underlying conditions					
Diabetes mellitus	1 (9.1)	1 (5.9)	2 (13.3)	1 (6.7)	n.s.†
Hypertension	2 (18.2)	1 (5.9)	-	-	n.s.†
Chronic kidney disease	-	2 (11.8)	3 (20.0)	3 (20.0)	n.s.†
Dyslipidemia	-	2 (11.8)	3 (20.0)	2 (13.3)	n.s.†
Asthma	-	-	1 (6.7)	-	n.s.†
Hypothyroidism	-	1 (5.9)	-	-	n.s.†
Positive inhibitory anti-IFN- $\gamma$ auAb titre, n (%)	-	14 (82.4)	15 (100.0)	15 (100.0)	<0.0001‡

Values are presented as average  $\pm$  SE or number (%).

n.s., non-statistically significant.

\*Statistical differences were tested with one-way ANOVA; †Statistical differences between dNTM patients and healthy controls were tested with  $\chi^2$ .

(Fig. 1A). Moreover, the titers in patients with progressive clinical outcomes tended to be higher than in those with non-progressive infection, ( $p=0.05$ ; Fig. 1A). We then analyzed changes in auAb titers from the initial diagnosis (baseline) to the day of enrollment in this study (endline) (Fig. 1B). In inactive dNTM patients, mean titers of baseline samples fell into the range of 1,000–10,000 but had significantly decreased to 100–1,000 by the time of enrollment in the present study ( $p=0.0312$ ). All inactive dNTM-infected cases exhibited either stable or declining trajectories. Therefore, from the initial day of diagnosis, patients with an inactive state tended to exhibit lower auAb titers overtime. In active dNTM group, mean auAb titers at baseline in both non-progressive and progressive cases (exceeding 10,000) were remarkably higher than those observed in inactive dNTM infection (below 10,000). Dynamically, progressive active patients exhibited the increased auAb titers ( $p=0.0156$ ) and displayed either stable or increasing trajectories in all cases. In non-progressive active patients, while overall trend showed a decrease in titers over subsequent years ( $p=0.0244$ ), some individuals presented increasing levels. This variability complicates the accurate stratification of the auAb trajectories among active infection subgroups (Non-progressive Active vs. Progressive Active). However, despite the varying trajectories observed in non-progressive cases, auAb titers in all active dNTM cases remain significantly higher than those with inactive dNTM infections throughout the course of disease.

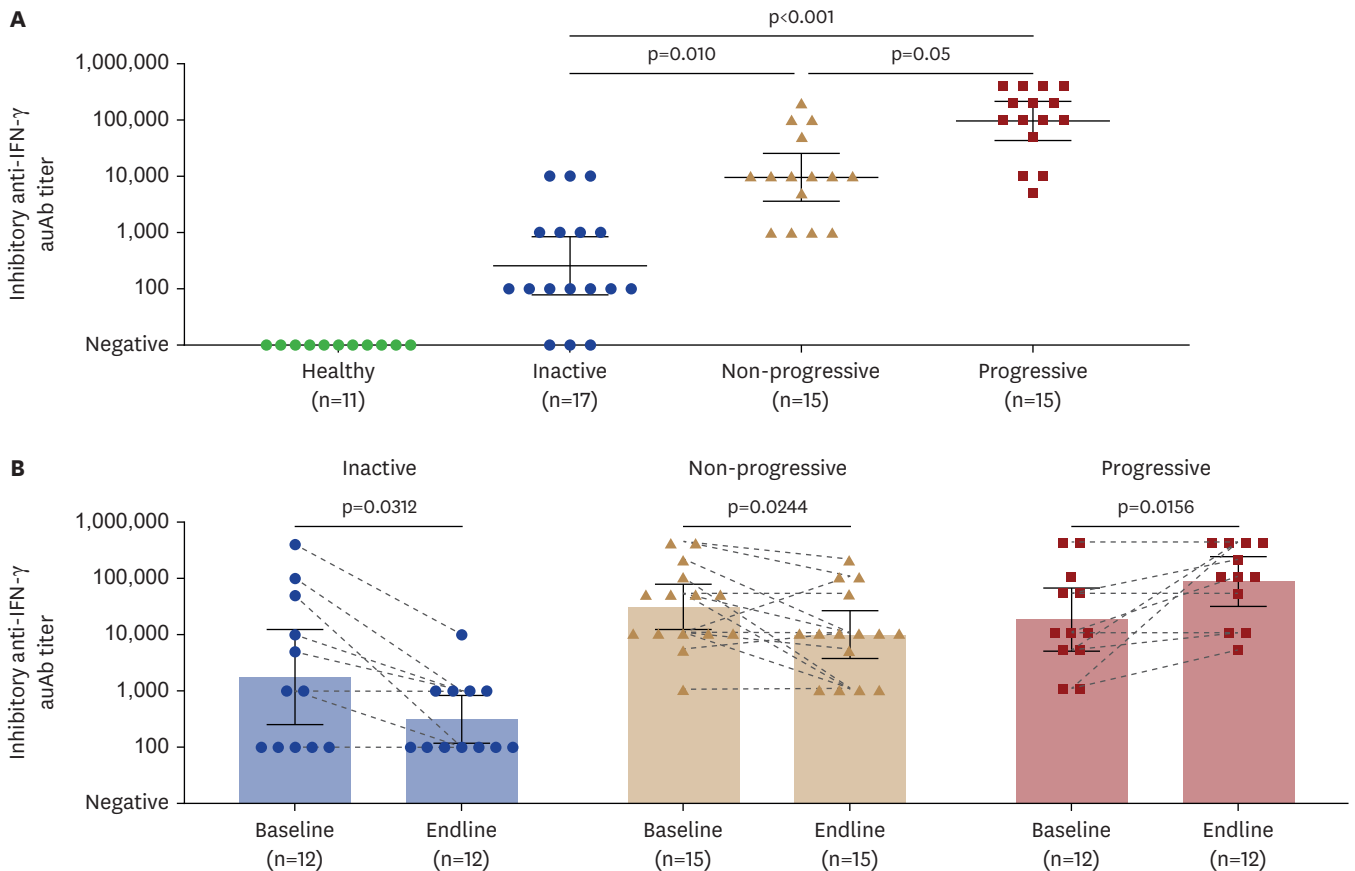


**Figure 1.** Comparison of plasma anti-IFN- $\gamma$  auAb inhibitory titers among participants in this study. (A) Anti-IFN- $\gamma$  auAb inhibitory titers at the current enrollment (endline) of healthy individuals, inactive, non-progressive active, and progressive active dNTM infections. Dot plots with horizontal lines of geometric means and 95% confidence intervals were shown. Statistical differences were tested using Kruskal-Wallis with Dunn's multiple-comparison tests. (B) Dynamics of anti-IFN- $\gamma$  auAb inhibitory titers from the day of initial diagnosis (baseline) to the day of enrollment in the present study (endline). Dashed lines represent results from the paired sample measurements which were statistically tested using Wilcoxon matched pairs signed rank test. Significant differences were determined as  $p < 0.05$ .

### Different patterns of whole-blood transcriptome profiles of active dNTM infection compared to those with no sign of infection

To investigate the differences in gene expression by circulating leukocytes among patients with different clinical conditions and healthy controls, samples from 5 representative cases of each group were subjected to transcriptome profiling. The characteristics of the selected samples are shown in **Supplementary Table 1**. The Inactive Infection group comprised 3 cases with negative auAb titers and 2 cases with titers at 100. The Non-progressive Active group was comprised of 4 cases with titers at 10,000 and another case with a titer of 100,000. Finally, the Progressive Active group was comprised of 2 cases with titers at 10,000 and 3 cases with titers at 100,000, 200,000, and 400,000. The bioinformatics pipeline following RNA sequencing is shown in **Supplementary Fig. 1**. Principle component analysis (PCA) of all detectable genes showed clustering of healthy control and inactive dNTM patients, while patients with active infection appeared to form a separate cluster (**Fig. 2A**). Therefore, we decided to group healthy control and inactive dNTM patients together as “No signs of Infection” versus “Active Infection” (progressive and non-progressive dNTM) for some bioinformatics analyses.

We identified differentially expressed genes (DEGs) by comparing expression levels of genes in the “Active Infection” group to those in the “No signs of Infection” group. This identified 168 up-regulated and 164 down-regulated genes in patients with “Active Infection” (**Fig. 2B**). The PCA of DEGs clearly placed “Active Infection” and “No signs of Infection” samples in different clusters (**Fig. 2C**). An unsupervised heatmap analysis of the DEGs shows detailed expression levels of genes from each individual (**Fig. 2D**). This shows clear separation of gene-expression patterns in those with “Active Infection” from those with “No signs of Infection.”

### Over-expression of inflammatory responses, especially production of IL-8, in active dNTM infection

Pathway analysis of up- and down-regulated DEGs was then performed using two analysis tools: GO and Reactome pathways. Of the 168 up-regulated DEGs from active dNTM cases, the top ten GO terms of biological processes are shown in **Fig. 3A**. All top ten GO terms have the same significant adjusted p-value of 0.038. Interestingly, 5 of these pathways are associated with regulation of inflammatory cytokines, including: TNF-mediated signaling (GO:0010803); cytokine-mediated signaling (GO:0001959); response to cytokine stimulus (GO:0060759); positive regulation of IL-8 production (GO:0032757); and positive regulation of TNF-mediated signaling pathways (GO:1903265). Gene network analysis identified several pattern-recognition molecules encoding genes including *MRC1*, *NAIP*, *CD24*, *CRI*, and *TLR5* (**Fig. 3B**). Moreover, *HSPA1A* and *HSPA1B*, members of heat shock protein (HSP) family, were present in all top ten GO terms.

Analysis of gene expression via the Reactome database, identified that the most significant and prevalent pathways among the top 10 are related to cellular responses to stress which include the attenuation phase (R-HSA-3371568), and HSP/heat shock factor related pathways (R-HAS-3371571, R-HAS-3371497, and R-HAS-3371453) (**Fig. 3C**). In addition, the analyses identified that neutrophil degranulation (R-HSA-6798695) and extracellular signaling via G-protein coupled receptors (GPCRs; R-HSA-418594 and R-HSA-500792) are prominent among over-expressed DEGs (**Fig. 3C**). Within these three core pathways observed in active dNTM patients, gene network analysis revealed that HSP-encoding genes (*HSPA1A* and *HSPA1B*) were associated with neutrophil degranulation, while gene sets of extracellular signaling via GPCRs are separate from other pathways within the top ten Reactome pathways

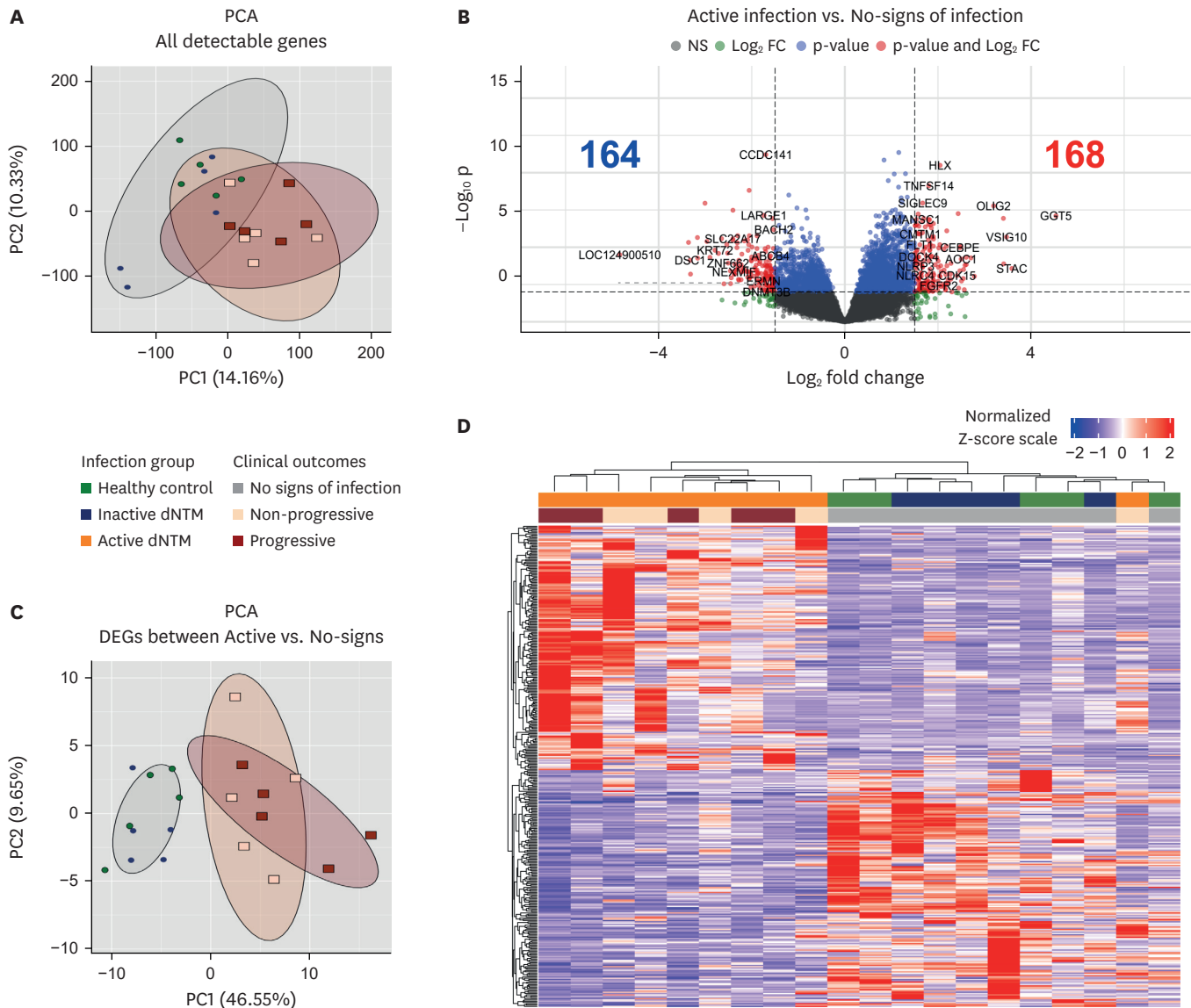


**Figure 2.** Whole-blood transcriptomic analysis to cluster responses among sample groups. (A) Data from representative samples (n=5 from each group) from healthy control (●), inactive dNTM (●), active non-progressive dNTM (●), and active progressive (■) dNTM were analyzed for similarity clustering by PCA. (B) Volcano plot shows DEGs between “Active Infection” versus “No signs of Infection” groups. DEGs were identified according to the criteria of read-count mean >10,  $p < 0.01$ , and  $-1.5 \leq |\log_2 \text{FC}| \geq 1.5$ . Numbers of both over-expressed and under-expressed genes according to these DEG criteria are as indicated. (C) PCA of DEGs shows clearly separate clusters between “Active Infection” and “No signs of Infection” groups. DEGs of each group are labelled as healthy control (●), inactive dNTM (●), active non-progressive dNTM (●), and active progressive (■) dNTM cases. (D) An unsupervised heatmap analysis of DEGs is shown with normalized Z-score of each gene (horizontal) from each sample (vertical). Data according to infection group (first clustering bar) are labelled as healthy control (■), inactive dNTM (■), “Active Infection” (■). Data according to clinical outcomes (second clustering bar) are labelled as “No signs of Infection” (healthy control and inactive dNTM group) (■), non-progressive (■), and progressive outcomes after treatment (■).

(Fig. 3D). These results suggest that neutrophil degranulation and cellular responses to stress are related to each other and are distinguished from the pathways of GPCR signaling. Supporting with the cell-type proportion analysis of our whole blood transcriptome using CIBERSORT revealed a significant increase in neutrophil responses (+42.1% relative percentage change) (Fig. 4A) when comparing the “No sign of Infection” group to the “Active Infection” group ( $p=0.0232$ ) (Fig. 4B).

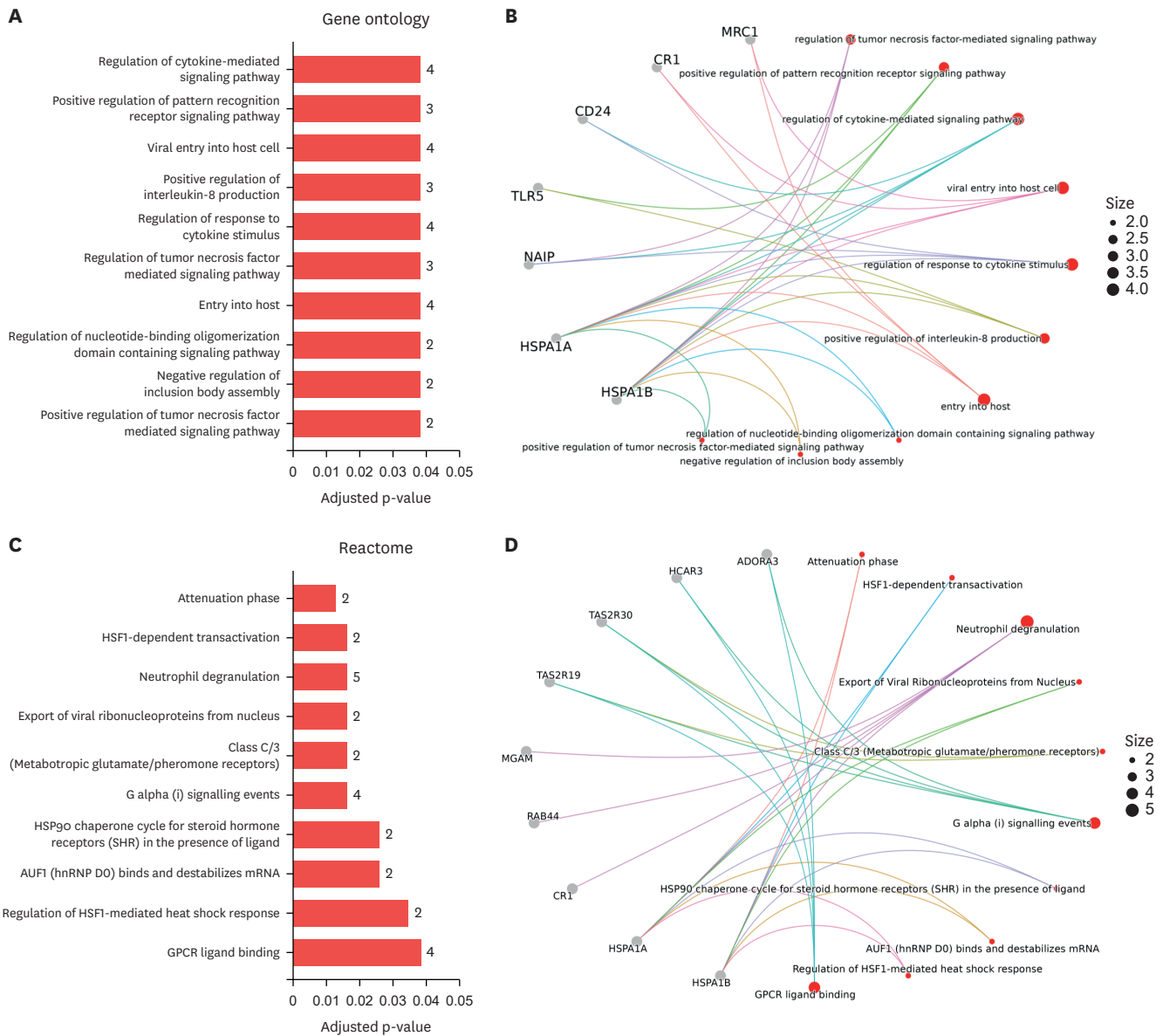


**Figure 3.** Differentially over-expressed pathways in the “Active Infection” group compared to those with “No signs of Infection.” Over-expressed DEGs were subjected to enriched pathway analysis. (A) Top ten GO terms in biological processes with adjusted p-value and number of gene counts within each term is indicated in each bar. (B) The interaction network of genes within each top ten GO terms. (C) Top ten pathways from the Reactome database with adjusted p-value and the number of gene counts within the pathway is indicated in each bar. (D) The interaction network of genes within each of the top ten Reactome pathways.

To confirm the observations from the whole-blood transcriptomics analysis regarding the overexpression of pro-inflammatory cytokines and neutrophil degranulation in patients with active dNTM infection, we measured IL-8 concentration in plasma from our patients and determined if levels were correlated with clinical conditions. **Fig. 5A** shows a significantly elevated IL-8 concentration in the plasma of the active dNTM patients compared to the inactive group ( $p=0.0167$ ). However, we found no significant correlation between plasma IL-8 levels and anti-IFN- $\gamma$  auAb titers ( $p=0.2225$ ,  $R^2=0.03363$ ) (**Fig. 5B**). Of the active dNTM patients, 6 cases had a history of neutrophilic dermatosis (ND) in previous visits, but not on the day of enrollment in this study. Four cases presented ND on the day of enrollment and all four had higher plasma IL-8 concentrations than those with a history of ND ( $p=0.0244$ ). Cases with no indication of ND demonstrated a broad range of IL-8 concentrations (**Fig. 5C**).

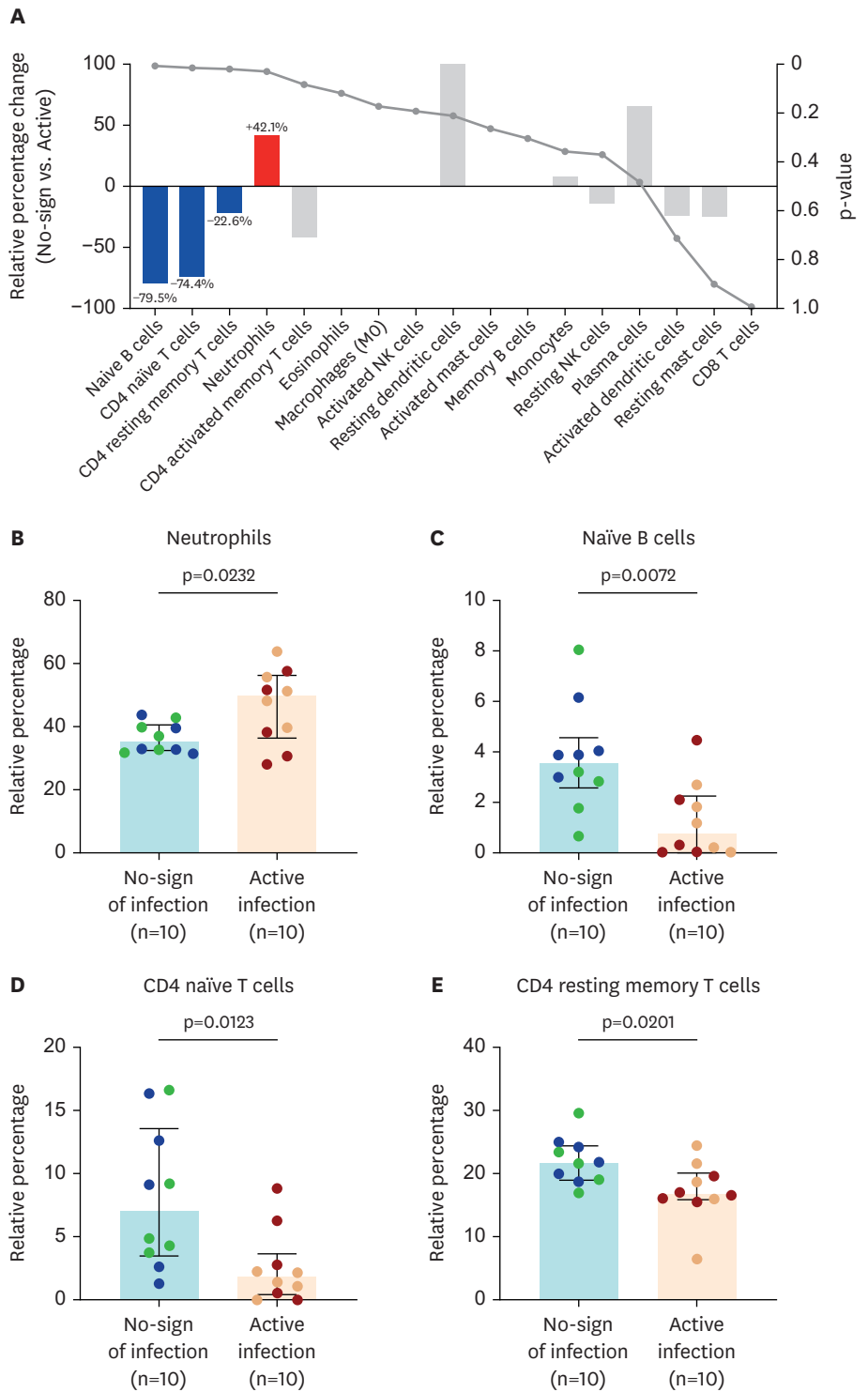


**Figure 4.** Estimation of cell-type fractions in bulk whole-blood RNA-seq data for the “Active Infection” group compared to those with “No signs of Infection.” The RNA-seq data was analyzed using CIBERSORTx for computational deconvolution. (A) Each cell-type fraction, along with its relative percentage change, is plotted on the left Y-axis, while p-values are plotted on the right Y-axis. Significant decreases are highlighted in blue, while increases are highlighted in red. (B-E) Dot plots with bars representing the median and interquartile range. Data from different groups are labeled as healthy control (●), inactive dNTM (●), active non-progressive dNTM (●), and active progressive dNTM cases (●). Statistical differences compared between groups were performed using unpaired t-tests.

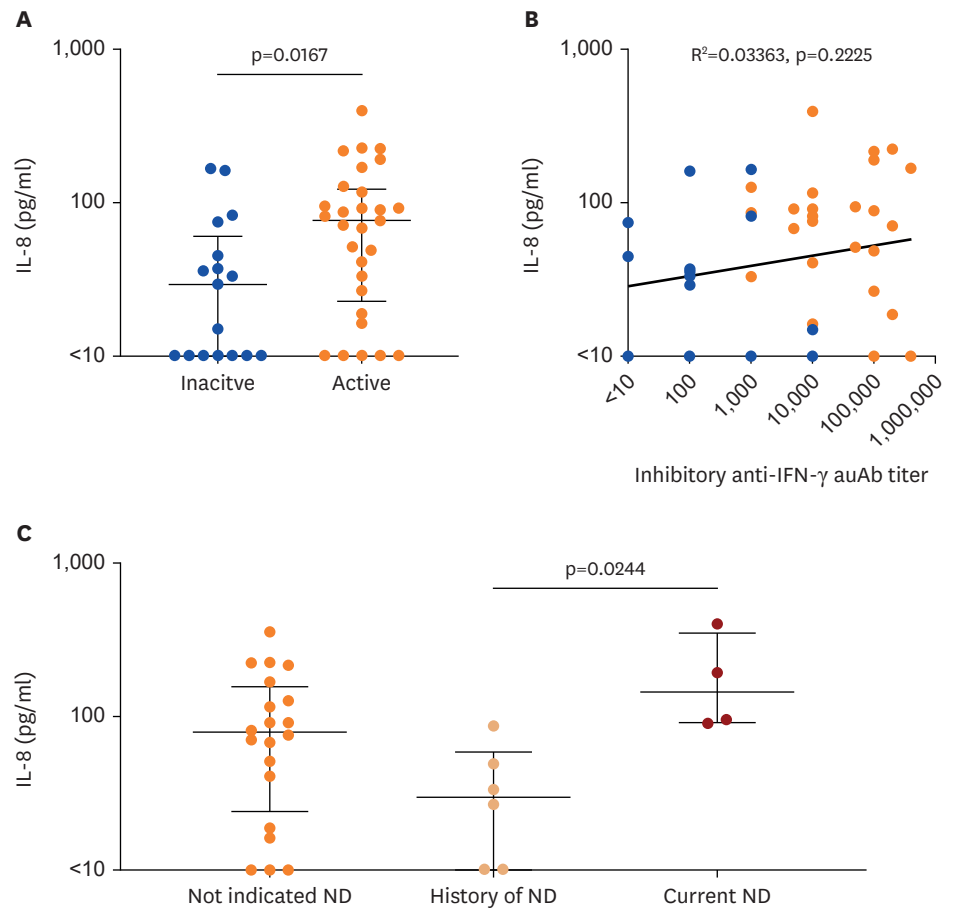


**Figure 5.** Plasma IL-8 concentration with its correlation with anti-IFN- $\gamma$  auAb inhibitory titers and the presence of neutrophilic dermatitis. Plasma IL-8 concentrations of 17 inactive and 29 active dNTM cases were measured by ELISA. (A) Dot plots with horizontal lines of median and interquartile range show plasma IL-8 concentrations from inactive (●) and active (●) dNTM cases. Statistical differences between inactive and active cases were analyzed using the Mann-Whitney test (B) Correlation analysis between plasma IL-8 concentration and plasma anti-IFN- $\gamma$  auAb inhibitory titers of both inactive (●) and active (●) dNTM cases were analyzed using linear regression. (C) Dot plots with horizontal lines of median and interquartile range of plasma IL-8 from active infection cases with no ND (●), with history of ND in past visit (●), and with current ND (●) on the day of enrollment in this study. Statistical differences compared among active dNTM cases with the presence of neutrophilic dermatitis were performed using one-way ANOVA with Kruskal-Wallis tests.

### Down-regulation of type-2 immune-response pathways in patients with active dNTM infections

The top 10 GO terms in biological processes of the 164 down-regulated DEGs from the active dNTM-infection group, are shown in **Fig. 6**. Five GO terms associated with immune responses were identified, including: response to LPS (GO:0032496); Type-2 immune response and its regulation (GO:0042092 and GO:0002828); and T cell cytokine production and its regulation (GO:0002369 and GO:0002724) (**Fig. 6A**). Interestingly, NLR family pyrin domain containing 3 (*NLRP3*) and arginase-1 (*ARG1*) were present in all GO terms related to immune responses, suggesting downregulation of inflammatory signaling via *NLRP3* inflammasome activation and alternatively activated macrophages, in patients with active dNTM infection (**Fig. 6B**). Other genes within the network (*CCR2*, *IL-1B*, *CLC*, *LEF1*) also support under-expression of macrophages and T cell-mediated responses.

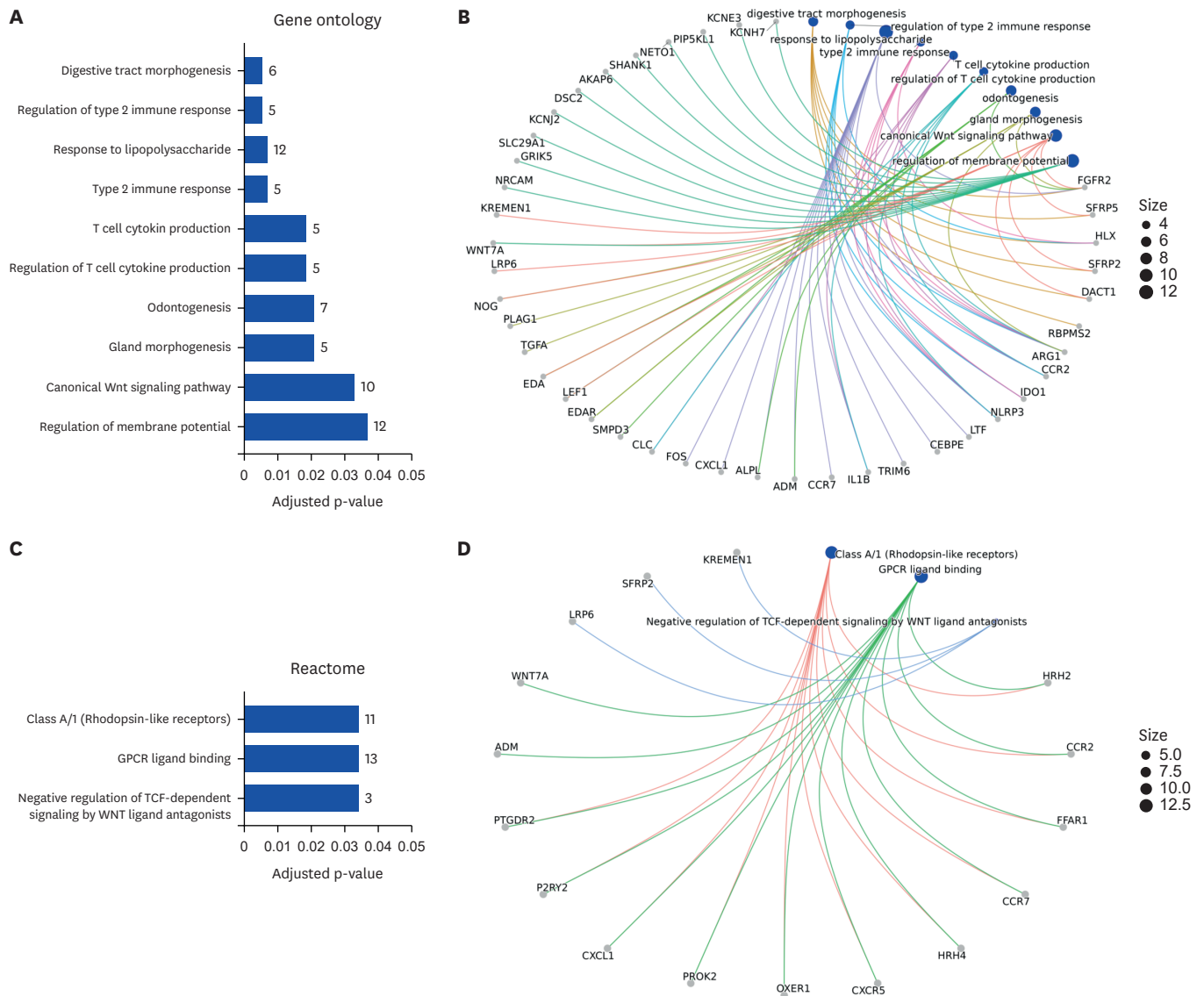


**Figure 6.** Differentially down-regulated pathways in the “Active Infection” group compared to the group with “No signs of Infection.” Under-expressed DEGs were subjected to enriched pathway analysis. (A) Top 10 GO terms in biological processes with adjusted *p*-value and gene counts within each term is indicated in each bar. (B) The interaction network of genes within each top ten GO term. (C) Top pathways from the Reactome database with adjusted *p*-value and gene counts within each pathway is indicated in each bar. (D) The interaction network of genes within each Reactome pathway.

Analysis using the Reactome database show significantly down-regulated pathways for: rhodopsin-like receptors (R-HSA-373076); GPCR ligand binding (R-HSA-500792); and negative regulation of T-cell factor (TCF)-dependent signaling by Wnt ligand antagonists (R-HSA-3772470) (**Fig. 6C**). Network analysis revealed that many DEGs within pathways of rhodopsin-like receptors and GPCR ligand binding are shared, but different genes exist within negative regulation of TCF-dependent signaling by Wnt ligand antagonists (**Fig. 6D**). Among the shared genes, most are receptor-encoding genes related to allergic inflammation (*PTGDR2*, *HEH4*, *HRH2*, *CXCR5*, *CCR7*, and *OXER1*), which support the findings via GO terms of under-expression and regulation of type-2 immune responses. Supporting with the cell-type proportion analysis showed a significant decrease naïve B cells (-79.5% relative percentage change), CD4 naïve T cells (-74.4% relative percentage change), and CD4 resting memory T cells (-74.4% relative percentage change) (**Fig. 4A**) when comparing the “No signs

of Infection” group to the “Active Infection” group ( $p=0.0072$ ,  $p=0.0123$ , and  $p=0.0201$ , respectively) (**Fig. 4C-E**).

### Possible biomarkers to differentiate progressive from non-progressive forms of active dNTM infection

We then compared gene expression between active dNTM patients with progressive infections versus non-progressive infections. In the former category, we identified 43 up-regulated and 20 down-regulated genes differentially expressed relative to the latter (**Fig. 7A**). In unsupervised heatmap analysis, sets of up- and down-regulated genes were differentially expressed in those with progressive disease and non-progressive disease (**Fig. 7B**). All 43 up-regulated DEGs in the progressive group are listed in **Supplementary Table 2** while the 20 down-regulated DEG are listed in **Supplementary Table 3**.

## DISCUSSION

The presence of circulating anti-IFN- $\gamma$  auAb, commonly recognized as AOID, worsens disease outcomes for dNTM patients. Our previous study showed the ability of anti-IFN- $\gamma$  auAb titers, measured by inhibitory ELISA, to differentiate dNTM patients with active clinical outcomes from inactive patients, using a titer cut-off at  $\geq 5,000$  with 92.7% sensitivity, 100% specificity, 100% positive predictive value and 76.9% negative predictive value (10). This study confirms and enhances our previous report that measurement of anti-IFN- $\gamma$  auAb levels is an effective diagnostic and monitoring tool for identifying patients with active infection, with substantial prognostic value. We show here that during the course of dNTM infection, there is a significant decrease in anti-IFN- $\gamma$  auAb in cases with inactive clinical outcomes and these changes in titers could help clinicians to monitor and predict the clinical improvement. A titer of less than 100 predicts the inactive stage of the disease, but larger studies and validation are required before this could be adopted into clinical practice. Among the active dNTM patients, anti-IFN- $\gamma$  auAb levels at the current enrollment (endline) tend to have a potential to distinguish ( $p=0.05$ ) those with progressive from those with non-progressive infections. In the dynamic analysis, elevated anti-IFN- $\gamma$  auAb titers were observed in progressive cases, but non-progressive cases showed unpredictable variation within the titer range of 1,000–100,000. Therefore, based on these findings, we conclude that the trajectories of anti-IFN- $\gamma$  auAb titers could not differentiate between active dNTM patients who progressed and those who did not. However, they could distinguish high auAb titers in the active stage from those in the inactive stage.

Our experiments employing whole-blood transcriptomics identified gene-expression patterns that can separate participants with active dNTM infection from those with no signs of infection (inactive dNTM infection and healthy individuals). DEGs demonstrated that i) upregulation of inflammatory cytokine-response pathways and ii) cellular pathways related to cell-stress conditions were associated with the active stages of dNTM infection. Conversely, type-2 immune responses were downregulated in these patients. These results suggest that inflammatory pathways are activated and that regulatory control mechanisms are impaired. Significantly, these predictions match the clinical observations for the role of an inflammatory phenotype in disease pathology.

The major clinical outcomes of dNTM infection include lymphadenopathy and reactive skin diseases (1,20) that are the result of overactive, persistent immune activation. Our data predict that IL-8 is likely to be a key player in immunopathology of this disease. IL-8

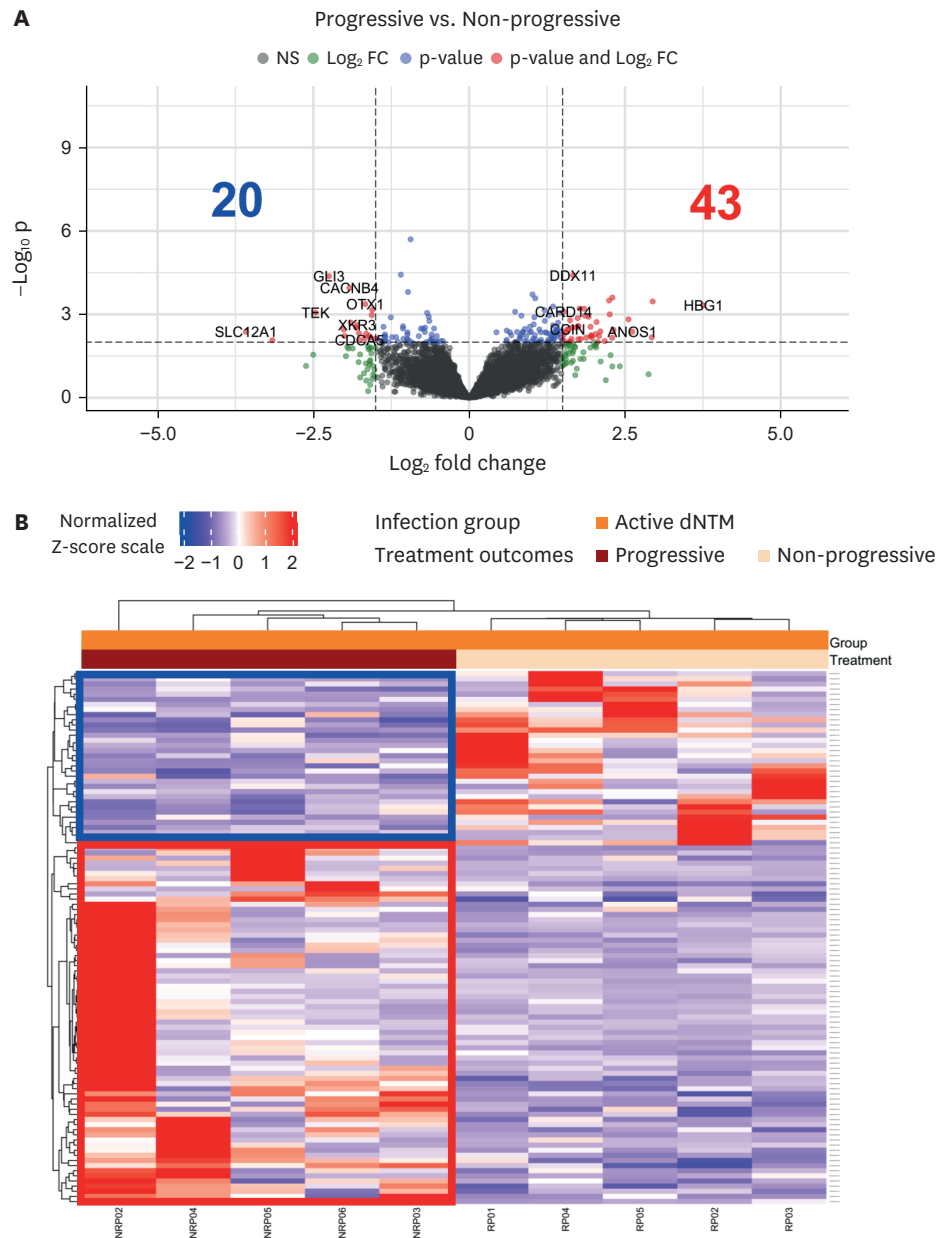


**Figure 7.** Significant DEGs of active infection cases with non-progressive disease versus patients with progressive disease after treatment. (A) Volcano plot shows DEGs between “Progressive Active” versus “Non-progressive Active” outcomes after treatment according to criteria of read count mean >10, p-value <0.01, and  $-1.5 \leq |\log_2FC| \leq 1.5$ . Numbers of both over- and under-expressed genes according to DEG criteria are as indicated. (B) An unsupervised heatmap analysis of DEGs showing normalized Z-score of each gene (horizontal) from each sample (vertical). Data from active infection cases (orange) were then classified as either progressive (red) or non-progressive (yellow) outcomes after treatment. Sets of up- and down-regulated genes that conversely differ between progressors and non-progressors are as square labelled of upregulation (-) and down-regulation (-).

potently attracts and regulates neutrophils (35). A significant elevation of plasma IL-8 in active dNTM infection compared to the inactive group confirmed our transcriptomic results. Interestingly, the potential of plasma IL-8 levels for discriminating patients with current neutrophilic dermatitis from patients with a prior history of neutrophilic dermatitis aligns with the disease pathogenesis caused by IL-8-mediated neutrophil activation and degranulation. Sweet syndrome, the most common skin disease among dNTM patients,

is associated with neutrophilic infiltrates in the dermis (1). Recently, marked increases of IFN- $\gamma$  and IL-17 in tissue, despite the presence of circulating anti-IFN- $\gamma$  auAb, have been proposed to be an inflammatory network enhancing aberrant neutrophil functions leading to immunopathology found in patients. (36). In the present study, we hypothesize that recruitment and activation of neutrophils within skin lesions are mediated by circulating IL-8, which is consistent with the evidence linking IL-8 as a predictor of neutrophil tissue infiltration in advanced cancer (37) and infectious diseases (38,39). High levels of IL-8 have also been observed locally in skin biopsies taken from patients with Sweet syndrome (40,41). Therefore, the significantly elevated levels of plasma IL-8, together with the whole-blood transcriptome profiles indicating a pro-inflammatory phenotype in active dNTM patients, could explain the pathogenesis of reactive skin diseases, especially Sweet syndrome.

Analysis of the predicted gene networks regulated in active dNTM patients, sheds new insights into potential pathological mechanisms. Among the over-expressed DEGs, pathways indicating cell stress and neutrophil degranulation (that are distinguishable from signaling through GPCRs) implies that neutrophil degranulation could additionally be amplified by cell-stress molecules, such as endogenous alarmins. HSP70 detected in the extracellular milieu are classified as damage-associated molecular patterns (DAMPs) (42) and HSP70 can induce Toll/IL-1 receptor signaling, subsequently activating innate immune cells (43). In the context of active dNTM infection, HSPs as DAMPs would serve as endogenous stimuli for immune activation. Thus, in synergy with IL-8, the cycle of neutrophil degranulation and inflammatory damage would be perpetuated.

GPCRs are versatile receptors that bind numerous extracellular signals to regulate a variety of cellular responses (44). The network of GPCR pathways with different sets of genes that are both over- and under-expressed DEGs could help identify the pattern of responses during disease progression. Our analyses of the up- and down-regulated GPCR pathways indicate that active dNTM infection might selectively induce neutrophil-mediated inflammation but suppress T cell-derived responses. IFN- $\gamma$ -primed mononuclear phagocytes and Th1 responses provide effective defense against mycobacteria (8,45). However, our data show downregulation of genes related to monocyte-derived macrophages, including *ARG1*, *IL-1 $\beta$* , monocyte chemoattractant protein-1 receptor (*CCR2*) and NLRP3 inflammasome (*NLRP3*), which indicates suppression of effector cells against NTM. These observations highlight the role of anti-IFN- $\gamma$  auAb in active dNTM patients in blocking IFN- $\gamma$ /IL-12 regulatory pathways, potentially leading to increased susceptibility to infection (6-8,46).

The anti-IFN- $\gamma$  auAb has been reported to be associated with opportunistic infections, particularly disseminated NTM (4,47). Binding of the auAb to a major epitope of IFN- $\gamma$  (amino acids 121-131) neutralizes downstream signaling of its receptor, leading to impaired antimicrobial responses (4,48,49). More recently, a clinical study of systemic lupus erythematosus patients with anti-IFN $\gamma$  auAb revealed an increased chance of severe infections (50). Our observations indicate that anti-IFN $\gamma$  auAb were present in all active dNTM cases and a significant proportion of inactive dNTM cases (14/17, 82.4%). We also observed increased responses from neutrophils while decreased responses from naïve B cells, CD4 naïve T cells, and CD4 resting memory T cells. This aligns with previous research on the immunophenotyping of NTM-infected patients with anti-IFN- $\gamma$  auAb, which demonstrated higher Ab-enhancing B cells, plasmablasts, and T helper 17 cells, while naive and regulatory T cells were decreased (51). Taken together, these findings suggest that immune responses in active dNTM patients are more likely to be pathogenic rather than protective against NTM.

Observations from this study indicate that both plasma anti-IFN- $\gamma$  auAb inhibitory titers and plasma IL-8 levels can discriminate between active dNTM patients and those with inactive infections. However, these 2 biomarkers are not correlated with one another (**Fig. 5B**). This suggests that determination of plasma IL-8 levels should not replace measurement of anti-IFN- $\gamma$  auAb inhibitory titers for dNTM diagnosis. Instead, measurement of plasma IL-8 levels could function as an additional laboratory test for the purpose of monitoring disease activity, although further validation is required for this practice to be adopted.

In our study, we have analyzed samples covering all disease stages (inactive patients, active-progressors, active non-progressors) and we also matched the cases before and after treatment, to record changes of anti-IFN- $\gamma$  auAb inhibitory titers over the course of treatment. This approach has enabled us to propose that anti-IFN- $\gamma$  auAb inhibitory titers could be used as prognostic indicators for disease reactivity and treatment outcomes, especially for cases of inactive infection. We observed fluctuations in anti-IFN- $\gamma$  auAb inhibitory titers in active non-progressors and propose that these may be caused by the heterogeneity of treatment periods. From our transcriptomic analyses, we predict that IL-8 could participate in the pathogenesis of reactive skin diseases observed in active dNTM patients. However, we are aware that our small sample size in each patient cohort for transcriptome profiling (n=5), together with the use of whole blood that may have varying numbers of white blood cells in different patients, may impact the robustness of our findings. For example, whole-blood analyses do not allow us to identify the source of IL-8. Nevertheless, our whole-blood transcriptomics data has shed important new insights into the pathogenesis of dNTM infection, particularly the match between the clinical correlations and our findings of IL-8-mediated neutrophilic dermatitis.

In conclusion, this study has revealed decreased plasma anti-IFN- $\gamma$  auAb inhibitory titers after treatment of inactive dNTM patients. This could assist clinicians in monitoring disease activity and decision-making for treatment options to improve patient outcomes and management. We also provided new insights into disease pathogenesis: increased IL-8 is proposed as the key inducer of neutrophils in generating reactive skin lesions, especially Sweet syndrome. This novel finding of the role for IL-8 may be used to inform therapy, for example indicating use of neutralizing Abs, or other therapeutic interventions to alleviate severe inflammation and immune-mediated pathology in active dNTM patients.

## ACKNOWLEDGEMENTS

This work was supported by the National Research Council of Thailand (NRCT) under contract no. N42A650205. We acknowledge the medical staffs at Srinagarind Hospital, Khon Kaen University, Thailand, for assisting and reviewing patient records. We would like to acknowledge Prof. David Blair for editing the manuscript via Publication Clinic KKU, Thailand.

## SUPPLEMENTARY MATERIALS

### Supplementary Table 1

General characteristics of 5 representative participants in each group for transcriptomic analyzes

**Supplementary Table 2**

List of 43 up-regulated DEGs compared between active infected patients with progressive disease versus non-progressive outcomes after treatment

**Supplementary Table 3**

List of 20 down-regulated DEGs compared between active infected patients with progressive disease versus non-progressive clinical outcomes after treatment

**Supplementary Figure 1**

Flowchart of bioinformatics pipeline for transcriptomic analyses in this study. After fastq files had passed the quality check and poor-quality removal process, the fastq files were used as input for preparation process, beginning with mapping by HISAT2 version 2.2.1. Homo sapiens GRCh38 (accession No. GCA\_000001405.28) was used as reference. Gene count was performed using featureCounts and htseq version 2.0.2 prior to the analysis via R studio by using package DESeq2. Data was visualized as heatmap and volcano plot.

**REFERENCES**

- Chetchotisakd P, Kiertiburanakul S, Mootsikapun P, Assanasen S, Chaiwarith R, Anunnatsiri S. Disseminated nontuberculous mycobacterial infection in patients who are not infected with HIV in Thailand. *Clin Infect Dis* 2007;45:421-427. [PUBMED](#) | [CROSSREF](#)
- Kim RD, Greenberg DE, Ehrmantraut ME, Guide SV, Ding L, Shea Y, Brown MR, Chernick M, Steagall WK, Glasgow CG, et al. Pulmonary nontuberculous mycobacterial disease: prospective study of a distinct preexisting syndrome. *Am J Respir Crit Care Med* 2008;178:1066-1074. [PUBMED](#) | [CROSSREF](#)
- Henkle E, Winthrop KL. Nontuberculous mycobacteria infections in immunosuppressed hosts. *Clin Chest Med* 2015;36:91-99. [PUBMED](#) | [CROSSREF](#)
- Patel SY, Ding L, Brown MR, Lantz L, Gay T, Cohen S, Martyak LA, Kubak B, Holland SM. Anti-IFN-gamma autoantibodies in disseminated nontuberculous mycobacterial infections. *J Immunol* 2005;175:4769-4776. [PUBMED](#) | [CROSSREF](#)
- Wongkulab P, Wipasa J, Chaiwarith R, Supparatpinyo K. Autoantibody to interferon-gamma associated with adult-onset immunodeficiency in non-HIV individuals in Northern Thailand. *PLoS One* 2013;8:e76371. [PUBMED](#) | [CROSSREF](#)
- Chi CY, Chu CC, Liu JP, Lin CH, Ho MW, Lo WJ, Lin PC, Chen HJ, Chou CH, Feng JY, et al. Anti-IFN- $\gamma$  autoantibodies in adults with disseminated nontuberculous mycobacterial infections are associated with HLA-DRB1\*16:02 and HLA-DQB1\*05:02 and the reactivation of latent varicella-zoster virus infection. *Blood* 2013;121:1357-1366. [PUBMED](#) | [CROSSREF](#)
- Kampmann B, Hemingway C, Stephens A, Davidson R, Goodall A, Anderson S, Nicol M, Schölvinck E, Relman D, Waddell S, et al. Acquired predisposition to mycobacterial disease due to autoantibodies to IFN-gamma. *J Clin Invest* 2005;115:2480-2488. [PUBMED](#) | [CROSSREF](#)
- Wu UI, Holland SM. Host susceptibility to non-tuberculous mycobacterial infections. *Lancet Infect Dis* 2015;15:968-980. [PUBMED](#) | [CROSSREF](#)
- Krisnawati DI, Liu YC, Lee YJ, Wang YT, Chen CL, Tseng PC, Lin CF. Functional neutralization of anti-IFN- $\gamma$  autoantibody in patients with nontuberculous mycobacteria infection. *Sci Rep* 2019;9:5682. [PUBMED](#) | [CROSSREF](#)
- Nithichanon A, Chetchotisakd P, Matsumura T, Takahashi Y, Ato M, Sakagami T, Lertmemongkolchai G. Diagnosis of NTM active infection in lymphadenopathy patients with anti-interferon-gamma autoantibody using inhibitory ELISA vs. indirect ELISA. *Sci Rep* 2020;10:8968. [PUBMED](#) | [CROSSREF](#)
- Chetchotisakd P, Anunnatsiri S, Nithichanon A, Lertmemongkolchai G. Cryptococcosis in anti-interferon-gamma autoantibody-positive patients: a different clinical manifestation from HIV-infected patients. *Jpn J Infect Dis* 2016;70:69-74. [PUBMED](#) | [CROSSREF](#)
- Aoki A, Sakagami T, Yoshizawa K, Shima K, Toyama M, Tanabe Y, Moro H, Aoki N, Watanabe S, Koya T, et al. Clinical significance of interferon-gamma neutralizing autoantibodies against disseminated nontuberculous mycobacterial disease. *Clin Infect Dis* 2018;66:1239-1245. [PUBMED](#) | [CROSSREF](#)

13. Chetchotisakd P, Anunnatsiri S, Nanagara R, Nithichanon A, Lertmemongkolchai G. Intravenous cyclophosphamide therapy for anti-IFN-gamma autoantibody-associated *Mycobacterium abscessus* infection. *J Immunol Res* 2018;2018:6473629. [PUBMED](#) | [CROSSREF](#)
14. Chaussabel D. Assessment of immune status using blood transcriptomics and potential implications for global health. *Semin Immunol* 2015;27:58-66. [PUBMED](#) | [CROSSREF](#)
15. Prebensen C, Lefol Y, Myhre PL, Lüders T, Jonassen C, Blomfeldt A, Omland T, Nilsen H, Berdal JE. Longitudinal whole blood transcriptomic analysis characterizes neutrophil activation and interferon signaling in moderate and severe COVID-19. *Sci Rep* 2023;13:10368. [PUBMED](#) | [CROSSREF](#)
16. Akthar M, Nair N, Carter LM, Vital EM, Sutton E, McHugh N, ; British Isles Lupus Assessment Group Biologics Register (BILAG BR) ConsortiumMASTERPLANS Consortium, Bruce IN, Reynolds JA. Deconvolution of whole blood transcriptomics identifies changes in immune cell composition in patients with systemic lupus erythematosus (SLE) treated with mycophenolate mofetil. *Arthritis Res Ther* 2023;25:111. [PUBMED](#) | [CROSSREF](#)
17. Gandhi KS, McKay FC, Cox M, Riveros C, Armstrong N, Heard RN, Vucic S, Williams DW, Stankovich J, Brown M, et al. The multiple sclerosis whole blood mRNA transcriptome and genetic associations indicate dysregulation of specific T cell pathways in pathogenesis. *Hum Mol Genet* 2010;19:2134-2143. [PUBMED](#) | [CROSSREF](#)
18. Parnell GP, McLean AS, Booth DR, Armstrong NJ, Nalos M, Huang SJ, Manak J, Tang W, Tam OY, Chan S, et al. A distinct influenza infection signature in the blood transcriptome of patients with severe community-acquired pneumonia. *Crit Care* 2012;16:R157. [PUBMED](#) | [CROSSREF](#)
19. Panousis NI, Bertsias GK, Ongen H, Gergianaki I, Tektonidou MG, Trachana M, Romano-Palumbo L, Bielser D, Howald C, Pamfil C, et al. Combined genetic and transcriptome analysis of patients with SLE: distinct, targetable signatures for susceptibility and severity. *Ann Rheum Dis* 2019;78:1079-1089. [PUBMED](#) | [CROSSREF](#)
20. Kiratikanon S, Phinyo P, Rujiwetpongstorn R, Patumanond J, Tungphaisal V, Mahanupab P, Chaiwarith R, Tovanabutra N, Chiewchanvit S, Chuamanochan M. Adult-onset immunodeficiency due to anti-interferon-gamma autoantibody-associated Sweet syndrome: a distinctive entity. *J Dermatol* 2022;49:133-141. [PUBMED](#) | [CROSSREF](#)
21. Nithichanon A, Samer W, Chetchotisakd P, Kewcharoenwong C, Ato M, Lertmemongkolchai G. Evaluation of plasma anti-GPL-core IgA and IgG for diagnosis of disseminated non-tuberculous mycobacteria infection. *PLoS One* 2020;15:e0242598. [PUBMED](#) | [CROSSREF](#)
22. Manbenmad V, So-Ngern A, Chetchotisakd P, Faksri K, Ato M, Nithichanon A, Lertmemongkolchai G. Evaluating anti-GPL-core IgA as a diagnostic tool for non-tuberculous mycobacterial infections in Thai patients with high antibody background. *Sci Rep* 2023;13:18883. [PUBMED](#) | [CROSSREF](#)
23. Bolger AM, Lohse M, Usadel B. Trimmomatic: a flexible trimmer for Illumina sequence data. *Bioinformatics* 2014;30:2114-2120. [PUBMED](#) | [CROSSREF](#)
24. Kim D, Paggi JM, Park C, Bennett C, Salzberg SL. Graph-based genome alignment and genotyping with HISAT2 and HISAT-genotype. *Nat Biotechnol* 2019;37:907-915. [PUBMED](#) | [CROSSREF](#)
25. Pott F, Postmus D, Brown RJ, Wyler E, Neumann E, Landthaler M, Goffinet C. Single-cell analysis of arthritogenic alphavirus-infected human synovial fibroblasts links low abundance of viral RNA to induction of innate immunity and arthralgia-associated gene expression. *Emerg Microbes Infect* 2021;10:2151-2168. [PUBMED](#) | [CROSSREF](#)
26. Liao Y, Smyth GK, Shi W. featureCounts: an efficient general purpose program for assigning sequence reads to genomic features. *Bioinformatics* 2014;30:923-930. [PUBMED](#) | [CROSSREF](#)
27. Anders S, Pyl PT, Huber W. HTSeq--a Python framework to work with high-throughput sequencing data. *Bioinformatics* 2015;31:166-169. [PUBMED](#) | [CROSSREF](#)
28. Love MI, Huber W, Anders S. Moderated estimation of fold change and dispersion for RNA-seq data with DESeq2. *Genome Biol* 2014;15:550. [PUBMED](#) | [CROSSREF](#)
29. Gu Z, Eils R, Schlesner M. Complex heatmaps reveal patterns and correlations in multidimensional genomic data. *Bioinformatics* 2016;32:2847-2849. [PUBMED](#) | [CROSSREF](#)
30. Yu G, Wang LG, Han Y, He QY. clusterProfiler: an R package for comparing biological themes among gene clusters. *OMICS* 2012;16:284-287. [PUBMED](#) | [CROSSREF](#)
31. Yu G, He QY. ReactomePA: an R/Bioconductor package for Reactome pathway analysis and visualization. *Mol Biosyst* 2016;12:477-479. [PUBMED](#) | [CROSSREF](#)
32. Robinson MD, McCarthy DJ, Smyth GK. edgeR: a Bioconductor package for differential expression analysis of digital gene expression data. *Bioinformatics* 2010;26:139-140. [PUBMED](#) | [CROSSREF](#)
33. Newman AM, Steen CB, Liu CL, Gentles AJ, Chaudhuri AA, Scherer F, Khodadoust MS, Esfahani MS, Luca BA, Steiner D, et al. Determining cell type abundance and expression from bulk tissues with digital cytometry. *Nat Biotechnol* 2019;37:773-782. [PUBMED](#) | [CROSSREF](#)

34. Newman AM, Liu CL, Green MR, Gentles AJ, Feng W, Xu Y, Hoang CD, Diehn M, Alizadeh AA. Robust enumeration of cell subsets from tissue expression profiles. *Nat Methods* 2015;12:453-457. [PUBMED](#) | [CROSSREF](#)
35. Baggiolini M, Walz A, Kunkel SL. Neutrophil-activating peptide-1/interleukin 8, a novel cytokine that activates neutrophils. *J Clin Invest* 1989;84:1045-1049. [PUBMED](#) | [CROSSREF](#)
36. Chieosilapatham P, Daroontum T, Suwansirikul S, Chaiwarith R, Phinyo P, Chaowattanapanit S, Choonhakarn C, Kiratikanon S, Rujiwetpongstorn R, Tovanabutra N, et al. Comparative immunohistochemical analysis of inflammatory cytokines in distinct subtypes of Sweet syndrome. *Front Immunol* 2024;15:1355681. [PUBMED](#) | [CROSSREF](#)
37. Schalper KA, Carleton M, Zhou M, Chen T, Feng Y, Huang SP, Walsh AM, Baxi V, Pandya D, Baradet T, et al. Elevated serum interleukin-8 is associated with enhanced intratumor neutrophils and reduced clinical benefit of immune-checkpoint inhibitors. *Nat Med* 2020;26:688-692. [PUBMED](#) | [CROSSREF](#)
38. Kaiser R, Leunig A, Pekayvaz K, Popp O, Joppich M, Polewka V, Escaig R, Anjum A, Hoffknecht ML, Gold C, et al. Self-sustaining IL-8 loops drive a prothrombotic neutrophil phenotype in severe COVID-19. *JCI Insight* 2021;6:e150862. [PUBMED](#) | [CROSSREF](#)
39. Kraft R, Herndon DN, Finnerty CC, Cox RA, Song J, Jeschke MG. Predictive value of IL-8 for sepsis and severe infections after burn injury: a clinical study. *Shock* 2015;43:222-227. [PUBMED](#) | [CROSSREF](#)
40. Marzano AV, Cugno M, Trevisan V, Fanoni D, Venegoni L, Berti E, Crosti C. Role of inflammatory cells, cytokines and matrix metalloproteinases in neutrophil-mediated skin diseases. *Clin Exp Immunol* 2010;162:100-107. [PUBMED](#) | [CROSSREF](#)
41. Marzano AV, Fanoni D, Antiga E, Quaglino P, Caproni M, Crosti C, Meroni PL, Cugno M. Expression of cytokines, chemokines and other effector molecules in two prototypic autoinflammatory skin diseases, pyoderma gangrenosum and Sweet's syndrome. *Clin Exp Immunol* 2014;178:48-56. [PUBMED](#) | [CROSSREF](#)
42. Asea A, Kraeft SK, Kurt-Jones EA, Stevenson MA, Chen LB, Finberg RW, Koo GC, Calderwood SK. HSP70 stimulates cytokine production through a CD14-dependant pathway, demonstrating its dual role as a chaperone and cytokine. *Nat Med* 2000;6:435-442. [PUBMED](#) | [CROSSREF](#)
43. Vabulas RM, Ahmad-Nejad P, Ghose S, Kirschning CJ, Issels RD, Wagner H. HSP70 as endogenous stimulus of the Toll/interleukin-1 receptor signal pathway. *J Biol Chem* 2002;277:15107-15112. [PUBMED](#) | [CROSSREF](#)
44. Hilger D, Masureel M, Kobilka BK. Structure and dynamics of GPCR signaling complexes. *Nat Struct Mol Biol* 2018;25:4-12. [PUBMED](#) | [CROSSREF](#)
45. Cowman SA, Jacob J, Hansell DM, Kelleher P, Wilson R, Cookson WO, Moffatt MF, Loebinger MR. Whole-blood gene expression in pulmonary nontuberculous mycobacterial infection. *Am J Respir Cell Mol Biol* 2018;58:510-518. [PUBMED](#) | [CROSSREF](#)
46. Xu C, Lu Z, Luo Y, Liu Y, Cao Z, Shen S, Li H, Liu J, Chen K, Chen Z, et al. Targeting of NLRP3 inflammasome with gene editing for the amelioration of inflammatory diseases. *Nat Commun* 2018;9:4092. [PUBMED](#) | [CROSSREF](#)
47. Chawansuntati K, Rattanathamthee K, Wipasa J. Minireview: Insights into anti-interferon- $\gamma$  autoantibodies. *Exp Biol Med (Maywood)* 2021;246:790-795. [PUBMED](#) | [CROSSREF](#)
48. Lin CH, Chi CY, Shih HP, Ding JY, Lo CC, Wang SY, Kuo CY, Yeh CF, Tu KH, Liu SH, et al. Identification of a major epitope by anti-interferon- $\gamma$  autoantibodies in patients with mycobacterial disease. *Nat Med* 2016;22:994-1001. [PUBMED](#) | [CROSSREF](#)
49. Saha B, Jyothi Prasanna S, Chandrasekar B, Nandi D. Gene modulation and immunoregulatory roles of interferon gamma. *Cytokine* 2010;50:1-14. [PUBMED](#) | [CROSSREF](#)
50. Chen L, Chi H, Teng J, Meng J, Zhang H, Su Y, Liu H, Ye J, Shi H, Hu Q, et al. Neutralizing anti-IFN- $\gamma$  IgG was increased in patients with systemic lupus erythematosus and associated with susceptibility to infection. *Clin Rheumatol* 2024;43:189-198. [PUBMED](#) | [CROSSREF](#)
51. Lee WI, Fang YF, Huang JL, You HL, Hsieh MY, Huang WT, Liang CJ, Kang CC, Wu TS. Distinct lymphocyte immunophenotyping and quantitative anti-interferon gamma autoantibodies in Taiwanese HIV-negative patients with non-tuberculous mycobacterial infections. *J Clin Immunol* 2023;43:717-727. [PUBMED](#) | [CROSSREF](#)